Available online at www.sciencedirect.com
ScienceDirect
Journal of Catalysis 243 (2006) 404–409
JOURNAL OF CATALYSIS
www.elsevier.com/locate/jcat

A theoretical study of coverage effects for ethylene epoxidation on Cu(111) under low oxygen pressure

Daniel Torres [a], Nuria Lopez [b], Francesc Illas [a,*]

[a] *Departament de Química Física & CeRQT, Universitat de Barcelona & Parc Científic de Barcelona, C/Martí i Franquès 1, E08028 Barcelona, Spain*
[b] *Institut Català d'Investigació Química (ICIQ), Departament de Química Física i Inorgànica, Universitat Rovira i Virgili, Avdga. Països Catalans 16, 43007 Tarragona, Spain*

Received 10 April 2006; revised 11 August 2006; accepted 16 August 2006

Abstract

The effect of oxygen coverage on the molecular mechanism of ethylene epoxidation on Cu(111) under ultra-high-vacuum conditions was studied by means of periodic density functional calculations. Oxygen coverages of 1/16 and 1/4 monolayer were considered. The results indicate that the barriers leading to ethylene oxide and acetaldehyde from a common oxametallacycle intermediate depend on the oxygen coverage. In particular, the decrease in the energy barrier leading to the epoxide with oxygen coverage can be correlated with a concomitant change in the formation energy of the desired product. It is also suggested that the optimum oxygen coverage for the epoxidation of a given olefin on Cu surfaces likely vary from one molecule to the other.

Keywords: Epoxidation; Ethene; Cu; Selectivity; Partial oxidation

1. Introduction

Epoxidation of small olefins is a technologically relevant reaction because epoxides are versatile intermediates for synthesis. For instance, ethylene oxide (EO), the simplest epoxide, is largely converted into ethylene glycol as well as many other derivatives. The industrial process is carried out exclusively using a silver catalyst consisting of silver particles supported on an inert alumina support [1]. To date, epoxidation has been the subject of many research studies [2,3], but most of the important advances in the development of epoxidation catalysts have been achieved through empirical means [4,5]. Based on stoichiometric reactions for the epoxidation reaction of various olefines carried out on Cu(111) and under ultra-high-vacuum (UHV) conditions, Lambert et al. suggested that the common belief that silver behaves as a unique catalyst should be revised [6,7]. Under UHV conditions, the study of ethylene epoxidation is elusive, and thus larger molecules containing the same functional group are used instead. This is the reason why most of the reactivity studies under UHV conditions are performed on styrene, which is a convenient chemical analog for ethylene. Lambert et al. have provided compelling evidence that for stoichiometric reactions involving styrene epoxidation, the reaction on Cu(111) leads to the desired products with an enhanced selectivity. Indeed, this selectivity appears to be strongly dependent on the oxygen coverage on the surface.

For epoxidation reactions occurring on Ag(111) surfaces, and even for partially oxidized silver surfaces, the molecular mechanism is known in detail [8–11]. Briefly, recall that it involves the reaction of ethylene with adsorbed oxygen through a partial oxidation route to form either EO or acetaldehyde from a common oxametallacycle (OMME) intermediate. The reaction scheme is

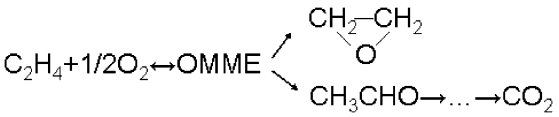

Recent theoretical work has suggested that the better performance of Cu under extremely low oxygen partial pressure is due to a significantly more favorable energy barrier difference

* Corresponding author.
E-mail address: francesc.illas@ub.edu (F. Illas).

0021-9517/$ – see front matter
doi:10.1016/j.jcat.2006.08.011

for the competing steps starting at the common oxametallacycle intermediate and leading to acetaldehyde and epoxide, respectively [12]. However, the reason for the dependence of selectivity on oxygen coverage remains unknown. To investigate the origin of this effect, density functional calculations were carried out for representative periodic models of the reaction between ethylene and oxygen on Cu(111) at different oxygen coverages. In this paper we present evidence demonstrating the influence of oxygen coverage on the energy barrier leading to EO and acetaldehyde.

2. Computational details

The mechanism for ethylene epoxidation has been studied by means of first-principles calculations based on density functional theory (DFT) applied to slab models representing the Cu(111) surfaces. The Kohn–Sham equations were solved using the VASP package [13,14]. The monoelectronic wave functions of the valence electrons were expanded on a plane wave basis with a kinetic energy cutoff of 315 eV, with the inner electrons represented by the PAW [15] method. The exchange-correlation functional used to obtain the energy was the Perdew–Wang (PW91) implementation of the generalized gradient approach [16]. Minimum energy paths and transition state structures were resolved using the climbing image nudged elastic band method (CINEB) [17]. The Cu(111) surface was modeled by a slab containing four atomic layers interleaved with five equivalent vacuum layers (∼10 Å).

To study the effect of oxygen coverage in the reaction path, two different supercells were used, in which the two fragments were adsorbed and the bimolecular reaction occurred. The first supercell was a $p(2 \times 2)$ cell containing 16 Cu atoms with both ethylene and oxygen adsorbed on the surface. The coverage of both oxygen and ethylene—and, therefore, of all the intermediates and products—was 0.25 ML. The second model involved a larger $p(4 \times 4)$ supercell containing 64 Cu atoms. This allows study of the reaction with 1/16 ML coverage for all species. For the $p(4 \times 4)$ supercell, a mixed 1/16 ML of ethylene and 0.25 ML of oxygen was also investigated. For calculation with the $p(2 \times 2)$ supercell, a Monkhorst–Pack [18] $4 \times 4 \times 1$ k-point mesh was used for integration in the reciprocal space. For the $p(4 \times 4)$ supercell, this was reduced to $2 \times 2 \times 1$. The reaction was studied by adsorbing the molecules just on one side of the slab; the resulting surface dipole was eliminated in the vacuum region [19]. These settings ensured that the adsorption energies converged to about 0.05 eV, whereas energy barriers were less affected by the technical details of the computation.

3. Results

3.1. Adsorption of oxygen and ethylene on Cu(111)

Oxygen adsorbs on threefold hollow sites with adsorption energies—calculated as $E_{\text{ads}} = \{E(\text{O} + \text{slab}) - \frac{1}{2}E(\text{O}_2) - E(\text{slab})\}$—of −1.56 for fcc sites and −1.64 eV for hcp sites, for the lowest coverage. Experimentally, the structure of the most stable adsorption site (fcc or hcp) remains unclear, at least for disordered patches of atomic oxygen on Cu(111) [20]. The elucidation of the hollow site responsible for atomic adsorption is a far from trivial task. With the present settings, the interaction of atomic oxygen on fcc or hcp is very close, slightly favoring the latter. However, recent work [21] has shown that using more stringent computational parameters reverses the order of stability, with the fcc adsorption site now slightly favored. However, these computational conditions cannot be used in the large supercell calculations reported in the present work. Indeed, we present evidence showing that the conclusions of this work do not depend on the active site chosen for atomic oxygen adsorption. Also note that the difference of adsorption energy for the two sites was too small to allow proper prediction, and other artifacts from the known inaccuracies of DFT in the proper assignment of the adsorption site also may play a role in determining the preferred adsorption site [22,23].

Table 1
Adsorption energies of atomic oxygen at different coverage with respect to molecular oxygen (O_2) and distances to the surface for the interaction with the high symmetry surface sites. Energies are in eV and distances in Å

	1/16 ML				1/4 ML			
	Top	Bridge	Fcc	Hcp	Top	Bridge	Fcc	Hcp
E_{ads}	−0.02	−1.23	−1.56	−1.64	0.16	−1.14	−1.44	−1.51
z	1.595	1.341	1.223	1.201	1.671	1.263	1.204	1.192

Table 1 gives the results for the geometry and adsorption energy for oxygen on the hcp site at the two different coverages defined above. This is the site selected for studying the reactivity toward epoxidation. The adsorption energy of oxygen on the –Cu(111) surface at the hcp site changed from −1.64 to −1.51 eV with increasing coverage from 1/16 and 1/4 ML, as expected based on the repulsion between negatively charged adsorbed oxygen atoms [24]. This in line with previous studies using a similar methodology [17]. For the coverage regime studied, oxygen adsorption induced modest changes in interlayer relaxation. At 1/16 ML, the interlayer relaxation for the first to second atomic layers (δ_{12}) was 0.5% and that for the second to third atomic layers (δ_{23}) was 0.2%; at 0.25 ML, these values increased (in absolute value) to 1.5 and 0.8%, respectively. However, the distance from the oxygen atom to the Cu surface atoms remained almost constant.

The adsorption of ethylene on Cu(111) was studied by temperature-programmed desorption (TPD), providing an adsorption energy of ∼0.30 eV [25]. This can be considered low adsorption energy. In fact, the low adsorption energy of ethylene is the reason why UHV experiments involving reaction of this species make use of larger molecular analogs, such as styrene, which exhibit greater adsorption energies. Vibrational frequencies for the adsorbed molecule measured using both reflection adsorption IR spectroscopy and EELS indicated that the molecule was adsorbed in the π-configuration, parallel to the surface and with a little distortion from the gas-phase structure [26]. Several initial adsorption sites were explored, depending on the adsorption site of each C atom. These sites include btb, tbt, tfcc, and thcp, corresponding to the situations where the two C atoms sit at bridge sites and the center of mass in a top site and where the C atoms sit at atop sites and the center

Table 2
Adsorption energy of ethylene on Cu(111) for a thcp arrangement and two different coverage. Energies are in eV, distances in Å, and angles in degrees

	1/16 ML	1/4 ML
E_{ads}	−0.10	−0.06
d_{CH}	1.093	1.095
d_{CC}	1.377	1.365
$d_{C_{top}Cu}$	2.334	2.241
$Angle_{HCCH}$	170.5	165.0

of mass at a bridge site or one C atom sits at a top site and the other atom sits at either at an fcc site or an hcp site.

The geometry optimization found stable structures in all cases, all of which had about the same adsorption energy. Here we must point out that the calculated adsorption energies are even smaller than the experimental ones. This is because of the well-known shortcomings of the present exchange correlation functionals, which do not incorporate dispersive forces. This may be considered a shortcoming of the present DF approaches, especially if the focus is on absolute adsorption energies. However, the effect is less important when the interest lies in energy differences. Because all stable structures exhibit similar adsorption energies, thcp was chosen for studying the epoxidation reaction. The calculated parameters for this structure in the two coverage situations are given in Table 2. For the thcp adsorption, there was virtually no difference in the structure of the adsorbed molecule at the two coverages, but again a slight decrease in adsorption energy from −0.10 to −0.06 eV can be predicted with increasing coverage from 1/16 to 1/4 ML, as expected from the long-range repulsive adsorbate–adsorbate interactions. The C atoms sat far away from the surface; C–C distances lay between gas-phase ethylene double-bond length of 1.334 Å and the value for gas-phase ethane double-bond length of 1.527 Å. The HCCH dihedral angle indicates the degree of distortion from the planar structure; it was 180° for free ethylene (Table 2). The C–C distance for adsorbed ethylene was ∼1.37 Å and the dihedral angle was ∼170°, indicating minor activation of the ethylene molecule. Accordingly, the C–C bond length and the HCCH dihedral angle can be used as measures of the double-bond activation. Our results on the structure of ethylene adsorbed on Cu(111) are in good agreement with the low adsorption energy on this surface.

3.2. Ethylene adsorption on oxygen precovered Cu(111)

Due to the low adsorption energy of ethylene to the clean Cu(111) surface, it is likely that under reaction conditions ($T > 500$ K), ethylene molecules will exhibit a very short residence time. However, increased adsorption energy for ethylene on oxygen-precovered Ag surfaces has been proposed based on calorimetric experiments [27] and on model calculations [28]. The theoretical study of the adsorption of ethylene on oxygen-precovered Cu(111) was carried out as follows. The oxygen atom was placed on a hcp threefold hollow site, and a geometry optimization was carried out for ethylene adsorbed near the oxygen. The starting geometry for adsorbed ethylene was the thcp site shown in Fig. 1; the presence of oxygen atoms

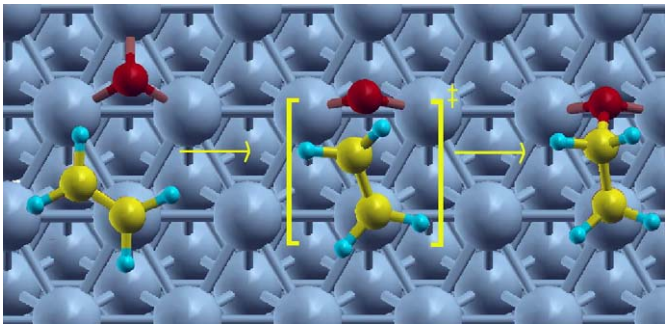

Fig. 1. Coadsorption of ethylene and oxygen on Cu(111) in the initial arrangement towards the formation of the OMME intermediate. Initial, transition, and final states.

on the surface favored ethylene adsorption in this case as well. This can be explained by the different electron donor–acceptor character of the reactants, the large negative charge on adsorbed oxygen facilitates donation to the π^* molecular orbital of ethylene. This implies that the sites with neighboring preadsorbed O atoms are the most favorable for ethylene adsorption. The binding energy of ethylene on the oxygen-precovered surface increased by ∼0.10–0.15 eV, and again in this case, the effect was larger at high dilutions; 0.14 eV gain for the 1/16 ML coverage, compared with 0.11 eV at greater coverage. Nonetheless, despite the greater donation capability of the oxygen-preadsorbed Cu(111) surface, the ethylene molecule remained only weakly activated, with the adsorbed ethylene geometry showing only slight distortion relative to the gas-phase molecule. For instance, the change in the C–C distance on adsorbing ethylene was ∼0.01 Å with respect to the gas phase. On the other hand, the presence of ethylene did not significantly affect the geometry of adsorbed oxygen, and the distance of oxygen to the surface remained unchanged.

3.3. Formation of the oxametallacycle

The greater adsorption energy and lower mobility of oxygen indicate that the mobile ethylene molecules are likely to approach adsorbed oxygen to start the reaction. An ethylene–oxygen interaction leads to the formation of the OMME intermediate similar to that reported for the reaction on Ag surfaces. The formation of this intermediate from the coadsorbed structure described above involves rotation of the ethylene molecule adsorbed on the thcp around an axis perpendicular to the surface and passing through the C atom sitting at the top site, reducing the C_{hcp}–O_{hcp} distance. This rotation activates the motion of O toward the nearest bridge site, further reducing this C–O distance. The geometry of the OMME intermediate and the adsorption energies with respect to gas-phase reactants for both coverages are shown in Table 3. The adsorption energy for the OMME intermediate was about −1.8 eV with respect to gas-phase reactants; the difference between the coverages again was small (about 0.07 eV), very similar to that found for reactants. In the final structure, the OMME sits with the O atom between two Cu atoms and the C–C bond midpoint is located over a hollow site. Coverage effects in the range of 1/16–1/4 ML did not affect the geometry of the intermediate, as indicated in the table.

Table 3
Adsorption parameters for O, C_2H_4 and for the oxametallacycle (OMME) intermediate corresponding to reaction of ethylene with oxygen on Cu(111) at different coverage. Ethylene was arranged on a thcp site while oxygen was adsorbed on an hcp site. The adsorption energies are given with respect to the O_2 molecule and ethylene in the gas phase. Energies are in eV and distances in Å

	1/16 ML					1/4 ML				
	E_{ads}	d_{OCu}	$d_{C_{top}}$	d_{CC}	$d_{C_{hcp}O}$	E_{ads}	d_{OCu}	$d_{C_{top}Cu}$	d_{CC}	$d_{C_{hcp}O}$
$C_2H_4 + O(ads)$	−1.64	1.912				−1.51	1.900			
$C_2H_4(ads) + O(ads)$	−1.84	1.895	2.849	1.345	3.186	−1.75	1.902	2.830	1.345	3.186
OMME(ads)	−1.86	1.991	2.024	1.518	1.457	−1.79	1.992	2.024	1.518	1.457

Table 4
Geometric parameters and energy barriers for the transition state involved in the OMME formation. Energies are in eV and distances in Å

	1/16 ML	1/4 ML
E^{TS}	0.63	0.64
$d_{C_{top}Cu}$	2.197	2.176
d_{CC}	1.394	1.423
$d_{C_{hcp}O}$	2.095	1.907

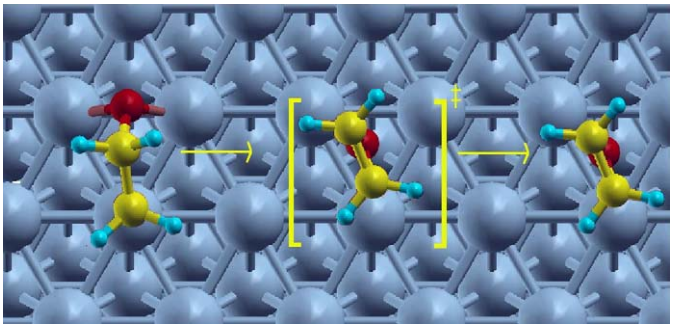

Fig. 2. OMME to epoxide reaction structures on Cu(111). Initial, transition, and final state.

The transition-state structure leading to the OMME is shown in Table 4. Along the resulting reaction path, the C–C bond was elongated from 1.345 Å in adsorbed ethylene to 1.394 Å at the TS and reaching 1.518 Å for the OMME species. While the C–O bond was being formed, the hybridization of the C atom interacting with oxygen changed from sp^2 to sp^3. This is evident from the change in the HCCH dihedral angle from ∼180° to 108° going through ∼156° at the TS structure. Simultaneously, the distance between oxygen and the metal went from 1.895 Å—in the coadsorbed oxygen and ethylene structure—to 1.991 Å for the final OMME state. For the 1/16 coverage, the TS structure lay 0.63 eV above the energy of coadsorbed oxygen and ethylene, whereas the OMME structure was 0.02 eV below this energy. In this case, coverage effects affected the C–C distance at the transition state structure, which was larger for the 1/4 ML case (see Table 4). However, the energy barrier for the reaction was almost unaffected, and for the 1/4 ML became 0.64 eV.

3.4. OMME to epoxide and acetaldehyde

From the OMME intermediate, two elementary reactions may occur, one leading to the desired product EO and another producing acetaldehyde. In any case, the final products are weakly adsorbed to the surface and thus easily desorb. Nevertheless, the two channels are qualitatively different despite leading to products that are stable with respect to the gas-phase reactants by 1.32 eV for the epoxide and 2.35 eV for acetaldehyde; the former lay above the energy of the OMME intermediate, whereas the latter lay below it. The geometric parameters of the products were almost identical to those corresponding to the gas-phase molecules and indeed insensitive to coverage, indicating no significant interaction between the adsorbed molecules.

Table 5
Geometric parameters and energy barriers for the transition state involved in the epoxide formation from the OMME intermediate. Energies are in eV and distances in Å

	1/16 ML	1/4 ML
E^{TS}	0.98	1.09
d_{CC}	1.461	1.461
$d_{C_{top}O}$	1.575	1.424

Table 6
Geometric parameters and energy barriers for the transition state involved in the acetaldehyde formation from the OMME intermediate. Energies are in eV and distances in Å

	1/16 ML	1/4 ML
E^{TS}	1.22	1.24
$d_{C_{top}Cu}$	2.210	2.439
d_{CC}	1.489	1.454
$d_{C_{hcp}H}$	1.170	1.288

Cycling the oxametallacycle to form the epoxide implies the formation of a bond between the O atom and the carbon directly bonded to the surface (Fig. 2). Consequently, the distance between the O atom and the surface increased while the C–O distance decreased. For the 1/16 and 1/4 ML coverages, one of the C–O distances went from 2.508 Å on the OMME to either 1.575 or 1.424 Å at the TS. Simultaneously, the C–C distance decreased from 1.518 to 1.461 Å at the TS structure; this distance is the same as for the free gas-phase molecule. The geometry for the transition state at both 1/16 and 1/4 ML coverage is reported in Table 5. The energy barrier for the OMME cycling to epoxide was 0.98 eV at low coverage and 1.09 eV at high coverage.

In parallel, the OMME can evolve to the formation of acetaldehyde (see Table 6). Following Linic and Barteau, the process can be understood as a 1,2-hydrogen shift, and the reaction coordinate can be followed by monitoring the C_{hcp}–H distance along the minimum reaction path (Fig. 3). In the OMME structure, this C–H distance was 1.108 Å, whereas at the TS it

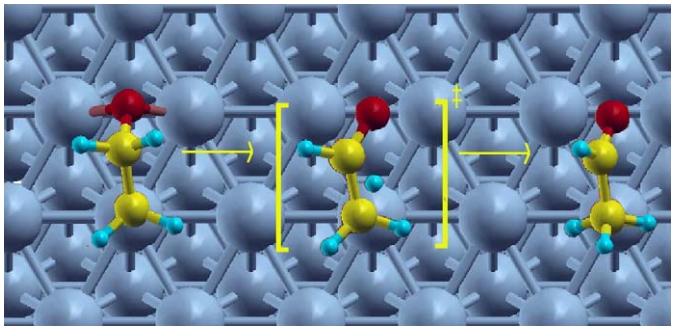

Fig. 3. OMME to acetaldehyde reaction structures on Cu(111). Initial, transition, and final state.

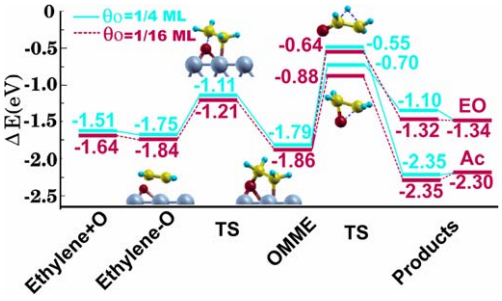

Fig. 4. Reaction profile and structures of epoxide and acetaldehyde formation starting from the coadsorbed reactants. (a) 1/4 ML (lighter lines and upper profile); (b) 1/16 ML coverage (darker lines and lower profile). Energies are referred to $\frac{1}{2}O_2$ and ethylene in the gas phase. The corresponding energy barriers are given in Tables 4–6.

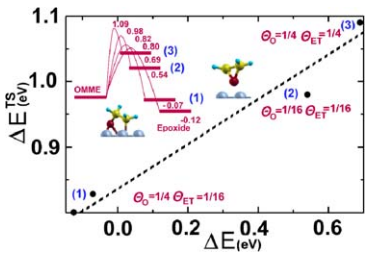

Fig. 5. Plot of the energy barrier from the OMME intermediate to the epoxide versus the relative energy of the product with respect to that of the OMME for three different coverage situations. For the situation represented as (1), two different arrangements for the adsorption of oxygen were considered (fcc and hcp sites). The dashed line connecting the calculated points is included to highlight the existence of a trend.

was 1.170 Å at 1/16 ML coverage and 1.288 Å at 1/4 ML coverage, with concomitant changes in the C–C distances from 1.518 to either 1.489 or 1.454 Å. However, although some geometry changes occurred depending on the coverage, the effect on the corresponding energy barrier was very small, 1.22 at 1/16 ML coverage and 1.24 eV at 1/4 ML coverage. Note that in contrast to what has been described for the TS leading to the epoxide, the structure of the TS leading to acetaldehyde on Cu(111) was rather independent of the surface coverage.

4. Discussion

To further investigate the effect of adsorbate coverage on the reaction profiles and energy barriers, the energy profiles for the two reaction channels and the two coverage situations considered in this work are summarized in Fig. 4. The analysis of these energy profiles shows that coverage effects were such that absolute values of the adsorption energies decreased with increasing coverage. However, the overall effect was quite small, because increasing the coverage by a factor of 4, from 1/16 to 1/4 ML, reduced the adsorption energy of reactants and OMME intermediate by only ∼0.1 eV. Moreover, this shift affected reactants and intermediates equally; thus, within the range studied, the thermodynamic energy profile of the first step of the molecular mechanism of the ethylene oxidation on Cu(111) was almost insensitive to the coverage.

But a different picture emerges when considering the overall energy profile. In the step leading to the OMME intermediate, the change in the energy barrier for the 1/16 and 1/4 ML was <0.01 eV. For the 1,2-H-shift from the OMME to acetaldehyde, the effect was very similar, although in this case, increasing the coverage within these limits increased the energy barrier by 0.02 eV. A completely different situation occurred for the elementary step going from the OMME intermediate to the epoxide final product. In this case, increasing the coverage incurred an increase in the corresponding energy barrier of 0.1 eV, which, being relative energy, is a meaningful quantity. A first conclusion arising from the sensitivity of energy barriers with coverage implies that a too-small unit cell may lead to artifacts in the energy barrier prediction.

To trace back the origin of the larger effect of coverage to the energy barrier leading to ethylene epoxide, we compared the geometries for the intermediate and transition states for the product formation for the two coverage situations. The differential surface average relaxation for the TS leading to acetaldehyde was noticeably larger for the 1/4 ML coverage (0.03 Å) than for the 1/16 coverage. The change in formation energy for the epoxide in the 1/4 and 1/16 ML situations, from 1.10 to 1.32 eV, was not found for acetaldehyde. To further investigate coverage effects, we carried out calculations for the 4×4 unit cell with a 1/16 ML coverage for ethylene but a 1/4 ML coverage for oxygen, considering the coadsorbed oxygen atoms in either fcc or hcp sites. The calculated energy barrier for the reaction from OMME to ethylene epoxide dropped to ∼0.8 eV, significantly smaller than that corresponding to the 1/16 or 1/4 ML coverage of both reactants. At the same time, the ΔE for reaction from OMME to EO reaction was more exothermic than in the previous cases (−0.07 eV, compared with 0.54 eV for 1/4 ML and 0.69 eV for 1/16 ML), and the effect of having coadsorbed oxygen on fcc on hcp sites was very small. This is clear from Fig. 5, which plots the energy barrier (E^{TS}) from the oxametallacycle to the epoxide transition state channel versus the energy difference between OMME and the adsorbed product. The trend in Fig. 5 seems to follow a Brønsted–Evans–Polanyi type relation, which suggests that stabilizing the epoxide with respect to the OMME results in a lower barrier for this step. Because of the different extensions of OMME and EO over the O-precovered surface, the local configurations of the preadsorbed O on the surface can modulate the relative OMME to EO stability and thus the barriers.

The foregoing discussion makes it clear that the present theoretical models predict a significant coverage effect in the molecular mechanism for ethylene epoxidation on Cu(111). This is in line with the results of Cowell et al. for butadiene epoxidation on Cu(111) mentioned above. The activity versus oxygen coverage plot shows a maximum in the range 0.05–0.1 ML. The present calculations for ethylene on Cu(111) also indicate that oxygen coverage will play an important role and suggest that the optimum oxygen coverage may be higher than that for butadiene epoxidation.

A final topic meriting further discussion is the endothermic character of the EO formation from OMME, although an increase in oxygen coverage decreases the energy difference. This implies that practical applications will have severe limitations in the contact times, because once epoxide is formed, the process can be reversed to the regeneration of OMME to lead to the thermodynamically favored acetaldehyde product. In any case, the major concern in a possible practical use of Cu is to avoid the formation of surface oxide, which recent first-principle thermodynamic studies predict to be the favored over a long range of conditions [29] provided that no reducing agents (like ethylene) are present.

5. Conclusion

Coverage effects in the ethylene epoxidation reaction on Cu(111) were studied for low (1/16 ML) and medium (1/4 ML) oxygen coverages. The adsorption energies of reactants, intermediates, and products are systematically affected by neighbor–neighbor interactions, thus implying no change in the overall thermodynamic profile. However, a significant differential effect of ∼0.1 eV in going from the 1/16 coverage model to the 1/4 coverage model occurred for the reaction barrier leading to ethylene epoxide but not for the elementary step leading to acetaldehyde by a 1,2-H-shift from the common OMME intermediate. Model calculations for a situation in which the oxygen coverage is greater than the ethylene coverage showed that preadsorbed oxygen also had an effect on the energy barrier leading to EO from the OMME intermediate. The decrease in this particular energy barrier was found to correlate with to the change in the reaction energy for this step and hence seems to follow a Brønsted–Evans–Polanyi-type relation. This is in agreement with the experimental observation that the selectivity toward the epoxide is largely influenced by oxygen coverage and suggests that the optimum oxygen coverage for the epoxidation of a given olefin on Cu surfaces may vary from one molecule to another.

Acknowledgments

The authors thank Professor R.M. Lambert for stimulating discussions and a careful reading of the manuscript. Financial support has been provided by the Spanish Ministry of Education and Science (projects CTQ2005-08459-CO2-01 and UNBA05-33-001) and the Generalitat de Catalunya (projects 2005SGR-00697, 2005 PEIR 0051/69 and Distinció per a la Promoció de la Recerca Universitària de la Generalitat de Catalunya to N.L. and F.I.). Some of the computer time was provided by the Centre de Supercomputació de Catalunya, CESCA, and Barcelona Supercomputing Centre, BSC, through generous grants from Universitat de Barcelona, Fundació Catalana per a la Recerca. D.T. thanks the Universitat de Barcelona for a predoctoral fellowship, and N.L. thanks the ICIQ Foundation for financial support.

References

[1] K. Weissermel, H.-J. Arpe, Industrial Organic Chemistry, VCH, New York, 1993.
[2] R.A. van Santen, H.P.C.E. Kuipers, Adv. Catal. 35 (1987) 265.
[3] D.J. Sajkowski, M. Boudart, Catal. Rev. Sci. Eng. 29 (1987) 325.
[4] R.M. Lambert, F.J. Williams, R.L. Cropley, A. Palermo, J. Mol. Catal. A 228 (2005) 27.
[5] J.G. Serafin, A.C. Liu, S.R. Seyedmonir, J. Mol. Catal. 131 (1998) 157.
[6] J.J. Cowell, A.K. Santra, R.M. Lambert, J. Am. Chem. Soc. 122 (2000) 2381.
[7] A.K. Santra, J.J. Cowell, R.M. Lambert, Catal. Lett. 67 (2000) 87.
[8] S. Linic, M.A. Barteau, J. Am. Chem. Soc. 125 (2003) 4034.
[9] M.-L. Bocquet, P. Sautet, J. Cerda, C.I. Carlisle, M. Webb, D.A. King, J. Am. Chem. Soc. 125 (2003) 3119.
[10] M.-L. Bocquet, D. Loffreda, J. Am. Chem. Soc. 127 (2005) 17207.
[11] S. Linic, M.A. Barteau, J. Am. Chem. Soc. 124 (2002) 310.
[12] D. Torres, N. Lopez, F. Illas, R.M. Lambert, J. Am. Chem. Soc. 127 (2005) 10774.
[13] G. Kresse, J. Hafner, Phys. Rev. B 47 (1992) 558.
[14] G. Kresse, J. Furthmuller, J. Phys. Rev. B 54 (1996) 11169.
[15] P.E. Blöch, Phys. Rev. B 50 (1994) 17953.
[16] (a) J.P. Perdew, J.A. Chevary, S.H. Vosko, K.A. Jackson, M.R. Pederson, D.J. Singh, C. Fiolhais, Phys. Rev. B 46 (1992) 6671;
(b) J.A. White, D.M. Bird, Phys. Rev. B 50 (1994) 4954.
[17] G. Henkelman, H. Jonsson, J. Chem. Phys. 113 (2000) 9978.
[18] H.J. Monkhorst, J.D. Pack, Phys. Rev. B 13 (1976) 5188.
[19] G. Kresse, J. Furthmüller, J. Comput. Mater. Sci. 6 (1996) 15.
[20] S.M. Johnston, A. Mulligan, V. Dhanak, M. Kadodwala, Surf. Sci. 519 (2002) 57.
[21] D. Torres, K.M. Neyman, F. Illas, Chem. Phys. Lett., in press.
[22] P.J. Feibelman, B. Hammer, J.K. Nørskov, F. Wagner, M. Scheffler, R. Stumpf, R. Watwe, J. Dumesic, J. Phys. Chem. B 105 (2001) 4018.
[23] A. Gil, A. Clotet, J.M. Ricart, G. Kresse, M. Garcia-Hernandez, N. Rosch, P. Sautet, Surf. Sci. 530 (2003) 71.
[24] P.S. Bagus, F. Illas, Phys. Rev. B 42 (1990) 10852.
[25] E. McCash, Vacuum 40 (1990) 423.
[26] R. Linke, C. Becker, Th. Pelster, M. Tanemura, K. Wandelt, Surf. Sci. 377 (1997) 655.
[27] C.-F. Mao, M.A. Vannice, Appl. Catal. A 122 (1995) 41.
[28] A. Kokalj, A. Dal Corso, S. de Gironcoli, S. Baroni, J. Phys. Chem. B 110 (2006) 367.
[29] A. Soon, M. Todorova, B. Delley, C. Stampfl, Phys. Rev. B 73 (2006) 165424.